

LIMNOLOGY and OCEANOGRAPHY



© 2024 The Authors. *Limnology and Oceanography* published by Wiley Periodicals L14.508

© 2024 The Authors. *Limnology and Oceanography* published by Wiley Periodicals L14.508

behalf of Association for the Sciences of Limnology and Oceanography.

doi: 10.1002/lno.12585

Seasonality of submarine groundwater discharge to an Arctic coastal lagoon

Emma J. Bullock , 1* Isabel V. Schaal, M. Bayani Cardenas, James W. McClelland, Paul B. Henderson, Matthew A. Charette

¹MIT-WHOI Joint Program in Oceanography/Applied Ocean Science and Engineering, Cambridge and Woods Hole, Massachusetts, USA

²Department of Geological Sciences, Jackson School of Geosciences, University of Texas at Austin, Austin, Texas, USA

Abstract

Supra-permafrost submarine groundwater discharge (SGD) in the Arctic is potentially important for coastal biogeochemistry and will likely increase over the coming decades owing to climate change. Despite this, land-to-ocean material fluxes via SGD in Arctic environments have seldom been quantified. This study used radium (Ra) isotopes to quantify SGD fluxes to an Arctic coastal lagoon (Simpson Lagoon, Alaska) during five sampling periods between 2021 and 2023. Using a Ra mass balance model, we found that the SGD water flux was substantial and dependent on environmental conditions. No measurable SGD was detected during the spring sampling period (June 2022), when the lagoon was partially ice-covered. During ice-free periods, the main driver of SGD in this location is wind-driven lagoon water level changes, not tides, which control surface water recirculation through sediments along the lagoon boundary. A combination of wind strength and direction led to low SGD fluxes in July 2022, with an SGD flux of $(6 \pm 3) \times 10^6 \,\mathrm{m}^3 \,\mathrm{d}^{-1}$, moderate fluxes in August 2021 and July 2023, which had an average flux of $(17 \pm 9) \times 10^6 \,\mathrm{m}^3 \,\mathrm{d}^{-1}$, and high fluxes in October 2022, at $(79 \pm 16) \times 10^6 \,\mathrm{m}^3 \,\mathrm{d}^{-1}$. This work demonstrates how soil and environmental conditions in the Arctic impact Ra mobilization, laying a foundation for future SGD studies in the Arctic and shedding light on the major processes driving Ra fluxes in this important environment.

Submarine groundwater discharge (SGD) is an important contributor of chemical species in many coastal settings (Moore 1996, 2008), yet is understudied in the Arctic (Lecher 2017). Two forms of SGD exist in the Arctic: subpermafrost SGD and supra-permafrost SGD. Sub-permafrost SGD inputs onto Arctic shelves have been investigated using heat flow modeling (Deming et al. 1992; Frederick

*Correspondence: ejbvt15@gmail.com

Additional Supporting Information may be found in the online version of this article.

This is an open access article under the terms of the Creative Commons Attribution-NonCommercial License, which permits use, distribution and reproduction in any medium, provided the original work is properly cited and is not used for commercial purposes.

Author Contribution Statement: E.J.B. laboratory experiments, collected field samples, processed samples, analyzed data, wrote the manuscript. I.V.S. collected field samples, processed samples, analyzed data. M. B.C. designed the research, collected field samples. J.W.M. designed the research, collected field samples, P.B.H. collected field samples, processed samples, analyzed data. M.A.C. designed the research, collected field samples, wrote the manuscript.

and Buffett, 2015) and radium (Ra) isotopes (Charkin et al. 2017). Supra-permafrost studies focus on the soil active layer, which seasonally thaws between spring and early autumn. Supra-permafrost SGD has recently been shown to be an important source of methane (Lecher et al. 2015), nutrients (Lecher et al. 2016), and dissolved organic matter (Connolly et al. 2020) to the coastal Arctic Ocean. Furthermore, it will become increasingly important in this region owing to amplified Arctic warming (IPCC 2021; Rantanen et al. 2022), which is leading to permafrost degradation, deeper active layers, and groundwater generation from melting ice.

For this study, we define SGD as the mix of fresh, brackish, and saline water originating from coastal sediments and discharging into nearby waters. Fluxes of SGD are often estimated using the four Ra isotopes (Moore 1996, 2008; Garcia-Orellana et al. 2021): 223 Ra ($t_{1/2} \sim 11.4$ d), 224 Ra ($t_{1/2} \sim 3.6$ d), 226 Ra ($t_{1/2} \sim 1600$ yr), and 228 Ra ($t_{1/2} \sim 5.75$ yr). As Ra isotopes are part of the U/Th decay series, they are sourced from crustal materials including rock and sediment. Ra sorbs strongly onto these materials under typical fresh groundwater conditions;

³The Ecosystems Center, Marine Biological Laboratory, Woods Hole, Massachusetts, USA

⁴Department of Marine Chemistry and Geochemistry, Woods Hole Oceanographic Institution, Woods Hole, Massachusetts, USA

Bullock et al.

however, upon encountering solutions of high ionic strength, Ra is released from sediment particles into the dissolved phase. This leads to brackish or saline SGD being enriched in Ra compared with inputs from rivers or other sources (Moore and Krest 2004), making Ra a useful tracer for SGD in coastal systems.

Given the heterogeneity of Arctic coastlines, Ra isotopes provide a way to integrate SGD inputs to a coastal system regardless of the driving forces. These can include terrestrial hydraulic gradients, wave setup and tidal pumping, flow-, and topography-induced pressure gradients, wave pumping, benthic exchange caused by bioirrigation or pressure differentials, and density-driven convection (Moore 2010; Santos et al. 2012). In Arctic systems with continuous permafrost and limited tidal range, wind-driven water level changes (Guimond et al. 2023) and the depth of the seasonally thawed active layer (Dimova et al. 2015) have been shown to be dominating forces controlling SGD fluxes. Of the few Arctic supra-permafrost SGD studies published to date, all took place during summer months and only one utilized Ra isotopes (Lecher et al. 2015). The complex physics and chemistry associated with this environment means that questions remain regarding the magnitude of Arctic SGD. To fill this knowledge gap, this study has three goals: (1) to characterize the sources and sinks of Ra isotopes in an Arctic lagoon system, (2) to estimate SGD fluxes to an Arctic coastal lagoon, and (3) to explore seasonal and interannual differences in Ra isotope distributions and SGD fluxes that result from the unique seasonality in the Arctic.

Methods

Field site and sample collection

The study was conducted in Simpson Lagoon (Fig. 1), an $\sim 245~\rm km^2$ estuary with minimal tidal influence (< 15 cm tidal range) located on the Alaskan Beaufort Sea coastline, which is fringed by similar lagoons covering over half of its length. Simpson Lagoon's coastline is 89 km long, including the barrier island shorelines that face the interior of the lagoon. The lagoon is shallow (average depth ~ 2 m) with annual shorefast ice cover lasting 8–9 months per year (Hanna et al. 2018). The mainland coastline of the lagoon is characterized by a narrow sandy beach backed by peat-rich polygon tundra bluffs (1 m high) and underlain by continuous permafrost (Hanna et al. 2018).

The average summer active layer depth ranges from 25 to 100 cm with the top \sim 20 cm consisting of organic peat and mineral soils found at deeper depths (Déry et al. 2005). Annual precipitation is \sim 22.5 cm yr $^{-1}$ (USDA 2022). Major river inputs come from the Kuparuk River at the lagoon's easternmost end (USGS: 15875000 Colville R AT Umiat AK 2023), various small streams along the coastline, and the Colville River at the lagoon's westernmost end (USGS: Kuparuk R NR Deadhorse AK 2023). Narrow passages between barrier islands

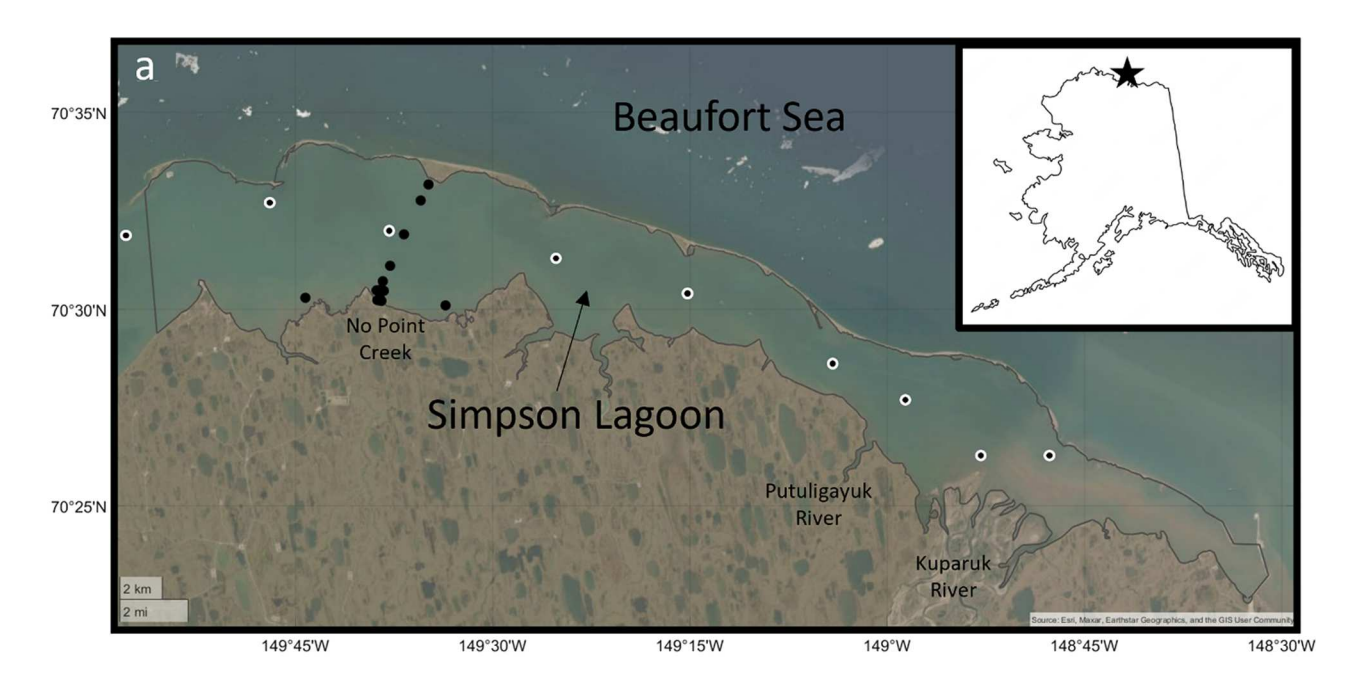
facilitate ocean-lagoon exchange, creating a semi-enclosed system.

Field campaigns and sampling were conducted during five different periods: spring (June 2022), summer (August 2021, July 2022, and July 2023), and autumn (September/October 2022). For all summer and autumn time periods, except for July 2023, lagoon surface samples were collected from a small boat in a shore-perpendicular transect (0.4, 0.8, 1.2, 1.6, 3.2, and 4.8 km from the mainland) at a depth of 0.5 m, with near-bottom samples collected at the three stations closest to shore and occasional extra stations sampled parallel to the shoreline. In July 2023, a full boat survey was conducted along the axis of the lagoon and in the surrounding Beaufort Sea (see Supporting Information Data S2) using the R/V Proteus. Samples were occasionally collected by hand (grab sampling) in the intertidal zone. Lagoon surface water Ra samples had a volume of $\sim 60 \, \text{L}$, collected via bilge pump and filtered through two in-line Hytrex cartridge filters (10 and $1 \mu m$). Samples collected from the R/V Proteus had volumes of \sim 70 L. The samples were weighed and filtered through a manganese coated acrylic fiber at a rate < 1 L per min. Salinity (S), dissolved oxygen (DO), temperature, turbidity, ORP, and pH were also measured with an AquaTROLL Multiparameter Sonde. Three rivers entering the lagoon were also sampled using the same hand collection technique: the Kuparuk River, the Putuligayuk River, and No Point Creek (see Supporting Information Data S3).

Groundwater sampling was designed to capture the heterogeneity of the field site, which included sandy beaches backed by either tundra bluffs or flat sand, tundra polygon wedges whose surrounding troughs create flow paths for fresh groundwater exiting the tundra, and subtidal areas with eroded peat interspersed with sandy sediment. Several shore-perpendicular transects of piezometers (4–12 stainless steel or PVC piezometers with six-inch-long screened intervals) were installed during each trip (Fig. 1), though not all piezometers were sampled for Ra each time. Transects were designed to traverse the subterranean estuary salinity gradient in all locations. Groundwater samples (0.5–30 L) for Ra isotopes were pumped from the piezometers directly through the Mn fiber column, which included a plug of uncoated acrylic fiber as a filter.

Sample analysis

Ra isotopes (²²⁴Ra, ²²³Ra, ²²⁶Ra, and ²²⁸Ra) were measured via the following set of procedures. After collection, fibers were rinsed with Ra-free deionized water to remove any particles or salt residue, and then partially dried so no water could be squeezed from the fiber. The short-lived isotopes ²²⁴Ra and ²²³Ra were measured within 2 d of sampling using RaDeCC delayed coincidence alpha detectors (Moore 2008). Supported ²²⁴Ra and ²²³Ra activities were determined by re-analyzing the fibers at 3 weeks and 2 months, respectively. Method efficiencies were determined using fiber standards spiked with known



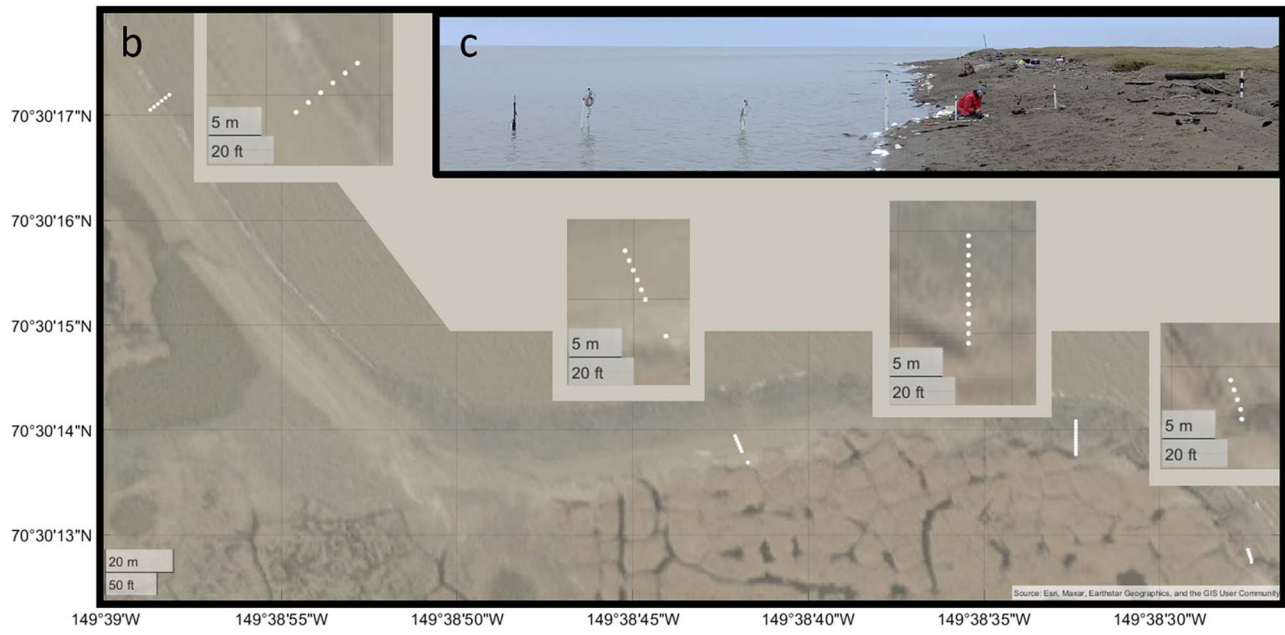


Fig. 1. Map of Simpson Lagoon. (a) Full lagoon with location along the Alaskan Beaufort coastline shown in insert and repeated surface water sampling stations shown in black dots. July 2023 interior lagoon sampling stations shown in black dots with white outline. See Supporting Information Data S1 for stations outside of lagoon. (b) Locations of shoreline piezometer transects. (c) Photograph depiction of a transect.

activities of ²²⁷Ac, ²³²Th, and ²²⁶Ra and analyzed using the same method as the samples (Scholten et al. 2010).

The long-lived isotopes were measured as follows: ²²⁶Ra was determined via the alpha scintillation technique described by Key et al. (1979). Briefly, fibers were placed in PVC housings, purged with helium, and then sealed for 3 weeks to ensure equilibrium between ²²⁶Ra and its daughter ²²²Rn. The ²²²Rn gas was collected by purging and cryo-trapping, and then transferred to an alpha scintillation (Lucas) cell. The cells

were analyzed on a radon counting system (Model AC/DC-DRC-MK 10–2). Method efficiencies were determined using fiber standards spiked with a known activity of 226 Ra (NIST SRM#4967A) and analyzed using the same method as the samples.

Finally, the fibers were combusted at 820°C for 8 h. The resultant ash was transferred to a polystyrene test tube and capped with epoxy before analysis for ²²⁸Ra on high-purity well-type germanium detectors using peaks for ²²⁸Ac (338 and

911 keV). In instances where $^{228}\mathrm{Ra}$ activities were too low to be counted using $^{228}\mathrm{Ac}$, samples were allowed to age for 6–12 months and $^{228}\mathrm{Ra}$ was then determined via $^{228\mathrm{Th}}$ ingrowth (238 keV). Select samples were also analyzed for $^{226}\mathrm{Ra}$ using this technique via $^{214}\mathrm{Pb}$ (352 keV). Detector efficiencies were determined using fiber standards that had been spiked with $^{226}\mathrm{Ra}$ and $^{232\mathrm{Th}}$ and then prepared in the same way as the samples.

Results

Surface water Ra activities

Surface water Ra activities are shown in Fig. 2, with averages and ranges given in Table 1. At the time of the June sampling, there were still 0.5–1.5 m of ice covering much of the lagoon. The sampled water, collected from the surface and through auger holes in the ice, was dominated by fresh meltwater. For a given sampling event, there was no notable surface water salinity gradient in the lagoon, though salinity varied dramatically seasonally and interannually.

Temperature and salinity measurements indicate that the lagoon was stratified during August 2021 and July 2022, with a fresher layer (0–1.7 m) overlying a saltier, colder bottom layer (> 1.7 m, approx. bottom depth \sim 2 m). Salinity profiles were taken at all surface water stations, with the range of salinity values shown in Table 1. The bottom layer had higher Ra activities, with all isotope activities being 40%–70%

higher than the top layer activities. These higher values can be explained by diffusion inputs into the bottom layer from Simpson Lagoon sediments (see Supporting Information Data S4). The Ra activities in the top layer of the lagoon for August 2021 and July 2022 were lower than those observed in the non-stratified periods of July 2023 or October 2022 (Table 1).

Groundwater Ra activities

Groundwater activities for each season are shown in Fig. 3 and in Table 1. All sampling periods exhibited strong heterogeneity in Ra activities, with outliers that were two to three standard deviations higher than the mean. The spring period had substantially higher Ra averages than the other periods, which had comparable activities (Table 1).

River Ra activities

Rivers can transport Ra to coastal waters in two ways: dissolved in river water and carried on suspended particles. The dissolved Ra activities in the Kuparuk River and Putuligayuk River were similar, with No Point Creek (reported as runoff) having slightly higher values (Table 1). Most Arctic rivers have not been sampled for short-lived isotopes; however, $^{226}{\rm Ra}$ activities measured in this study ranged between 1.4 and 3.9 dpm 100 L $^{-1}$, which are lower than those seen in large Arctic rivers such as the Yenisey and Lena Rivers in Siberia

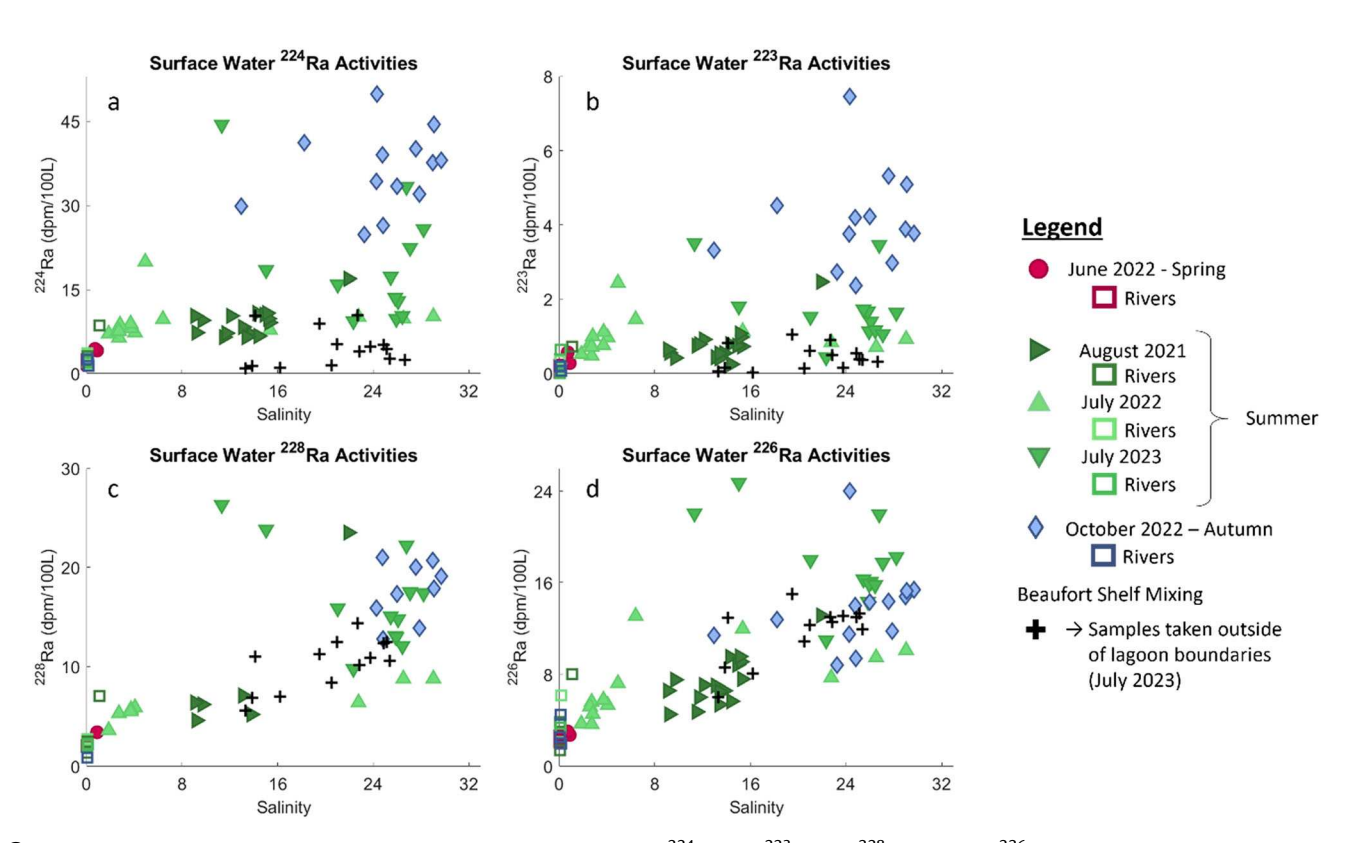


Fig. 2. Lagoon surface, river, and ocean Ra activities across seasons for (a) ²²⁴Ra, (b) ²²³Ra, (c) ²²⁸Ra, and (d) ²²⁶Ra.

Table 1. Isotope activities (dpm/100 L) and salinities across sampling periods.

Sample type	Sampling period	Salinity	²²⁴ Ra		²²³ Ra		²²⁸ Ra		²²⁶ Ra	
			Avg	Range	Avg	Range	Avg	Range	Avg	Range
Groundwater	June	0.1–62	42.3	3.3–189	3.5	0.08–19	17.7	8.3–35.3	7.0	0.52-38
	Aug 2021	0.6–18	8.6	0.4–72	0.5	0.0-4.8	10.8	2.7-24.3	2.9	0.4-22.9
	July 2022	0.3-29	16.7	1.0-125	1.4	0.0-11.0	_	_	2.6	0.7-9.6
	July 2023	0.6–20	19.8	1.6–155	1.1	0.0-7.6	12.0	1.1–105	15.3	3.4-130
	Oct 2022	0.5-36	13.9	0.7–72	1.1	0.03-6.4	10.8	7–15.6	4.9	0.9-13.6
Lagoon surface	June	2.6	4.1	3.9-4.4	0.36	0.22-0.57	_	_	2.87	2.71-3.02
water	Aug 2021	9–22	9.1	6.5-16.9	0.77	0.25-2.47	8.8	4.6-23.5	7.4	4.5-13.1
	July 2022	2–29	9.2	6.4–19.9	0.99	0.48-2.44	6.2	3.6-8.8	7.1	3.6-13.1
	July 2023	11–28	19.4	9.4-44.4	1.71	0.44-3.51	16.8	9.8-26.3	17.7	11.0–24.7
	Oct 2022	13-30	36.2	24.8-44.4	4.10	2.37-7.45	18.2	13.9-20.7	13.7	9.4–15.4
Rivers	All periods	>0.1	2.3	1.3-3.5	0.21	0.01-0.64	1.9	0.9-2.5	2.8	1.4-6.2
Runoff	All periods	0.1	3.7	1.6-8.6	0.25	0-0.70	4.9	2.7-7.0	4.2	2.3-8.0
Surface water from	July 2023	13–24	4.8	0.9-10.4	0.44	0.03-1.05	9.8	5.6-14.4	11.3	6.0-15.0
outside the lagoon		25-31	3.6	2.4-5.1	0.40	0.31-0.54	11.8	10.6-12.5	12.7	11.9–13.3

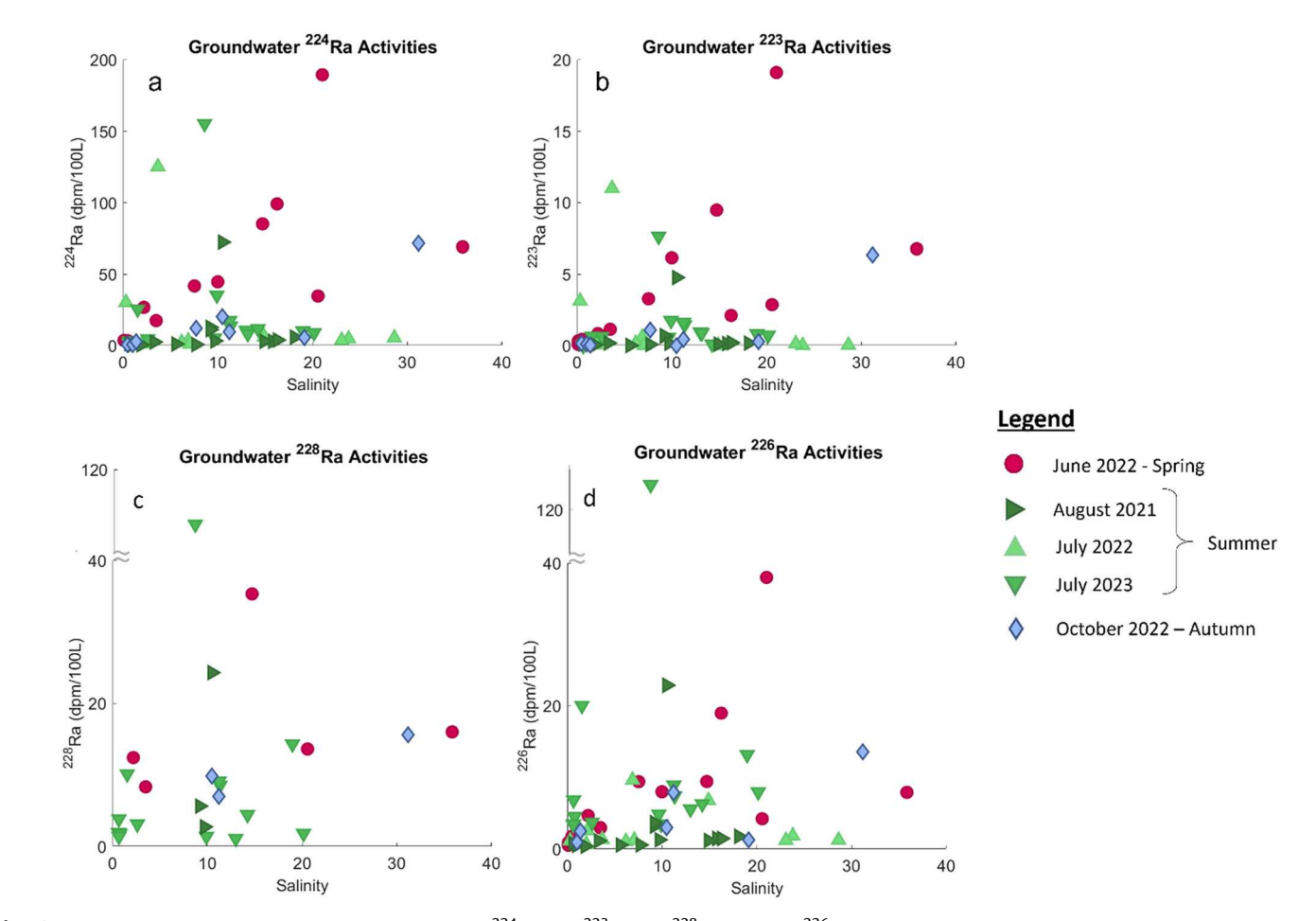


Fig. 3. Groundwater Ra activities across seasons for (a) ²²⁴Ra, (b) ²²³Ra, (c) ²²⁸Ra, and (d) ²²⁶Ra.

Bullock et al.

(Rutgers van der Loeff et al. 2003), or the Mackenzie and Yukon Rivers in North America (Kipp et al. 2020), but are comparable to activities seen in similarly sized Arctic rivers such as the Ellice River, rivers near Anchorage, AK (Bullock et al. 2022), and rivers in Greenland (Linhoff et al. 2020).

Riverine suspended sediments are also important, as ion-exchange-driven desorption can dominate riverine Ra inputs to coastal systems (Key et al. 1985). The desorption of Ra isotopes from Kuparuk River sediments was 0.09 ± 0.01 , 0.006 ± 0.002 , 0.07 ± 0.01 , and 0.08 ± 0.004 dpm g $^{-1}$ for 224 Ra, 223 Ra, and 226 Ra, respectively. Desorption experiments on Putuligayuk River sediment was not possible owing to loss of sample during transport. Discussion of desorption in a greater context can be found in the Supporting Information Data S3.

Discussion

Impact of wind direction on lagoon flushing

The lagoon water level varied by over 75 cm during our five sampling periods despite predicted tidal amplitudes of < 15 cm (Guimond et al. 2023). Guimond et al. (2023) show that this variability is owing to changing wind direction, with sustained winds from the east causing set-down periods of low water level. Such wind patterns increase wave action and cause the lagoon to oscillate between low and high-water levels (Guimond et al. 2023), allowing for increased benthic advective flow, the drainage of previously saturated, elevated sediments, and increased, wind- and wave-driven recirculation through lagoon sediments. Our data, as discussed in the following sections, support this conclusion and indicate that strong easterly winds increase mixing between the lagoon and the Beaufort Sea, as well as SGD-derived Ra within the lagoon.

Lagoon water Ra values are higher following wind-driven set-down periods, as seen in July 2023 and October 2022 (see wind visualization: Supporting Information Fig. S5). The highest values, seen during October 2022, were sampled immediately following a set-down period (Guimond et al. 2023). The lower Ra values from July 2023 were sampled several days after a set-down period (NOAA 2023), allowing the water level to begin rising back to its median value in the interim, which reduced the observed impact of the set-down period on the lagoon inventory. The salinities during these periods reflect higher mixing rates with the Beaufort Sea (Table 1; Supporting Information Table S3). In contrast, the sampling periods with stratification (August 2021 and July 2022) had lower surface salinities (Table 1) and lower percentages of wind coming from the east in the days leading up to sampling (see Supporting Information Fig. S5; NOAA 2023), although August 2021 still had higher wind speeds than those seen in July 2022 during surface water sampling. Winds from directions other than east therefore seem to allow the formation of a surface layer on the lagoon dominated by riverine inputs, while higher wind speeds still influence mixing between layers.

As the activity ratios (AR) of 224 Ra : 226 Ra are 1.4 ± 0.6 during August 2021 (S \sim 12.5), July 2022 (S \sim 3.6), and July 2023 $(S \sim 24.7)$ despite dramatically different salinities, it is unlikely that the ocean endmember is controlling Ra isotopes in the lagoon. In fact, the highest AR we observed was during the October 2022 sampling period (S \sim 27), when the 224 Ra: 226 Ra AR was 2.7 \pm 0.3. Owing to the short half-life of ²²⁴Ra, it tends to be depleted in deeper ocean waters compared with shallow coastal systems (Moore 1998), as seen in the stations we sampled immediately outside of the lagoon (AR $\sim 0.4 \pm 0.2$). Instead, the higher AR speaks to an increase in short term processes, such as wave pumping and advective flow through sediments, which are not long enough to allow ingrowth of the long-lived isotopes (Michael et al. 2011). This points to SGD as driving high lagoon Ra inventories during periods of set-down.

Processes driving groundwater Ra variations

During the spring sampling period, the ground was still mostly frozen, with landfast ice along the shore. Groundwater had thus been in contact with the surrounding soil since the autumn period of the previous year. This longer residence time likely enriched the groundwater in Ra (Michael et al. 2011).

For all periods sampled, Ra activities showed minimal dependence on salinity, which is unusual given Ra has been shown to be enriched in brackish and saline groundwater owing to competing cations interfering with Ra²⁺ adsorption onto solids (Webster et al. 1995; Gonneea et al. 2008; Beck and Cochran 2013). No associations with other measured parameters (pH, DO, ORP, and temperature) were found that might explain these deviations; however, field observations and hydrological measurements revealed strong heterogeneity within the coastal sediments, with erosion and storm overtopping intermittently burying large, intact chunks of peat. Preferential flow paths and pooling were observed, potentially causing varied groundwater residence times within several square meters. Samples with different residence times but the same salinity will presumably have different Ra activities (Michael et al. 2011).

The ice-free season (summer and autumn) Ra activities in Simpson Lagoon groundwater exhibit lower averages compared with other, more temperate sites (Charette et al. 2001), likely owing to factors impacting the solid/solution partitioning coefficient ($K_{\rm d}$) of Ra. In a comparable site along the Beaufort Sea coastline, the carbon content of tundra soils averaged 12% (Bristol et al. 2021)—sediments with high organic matter content have a large adsorptive capacity for Ra and are capable of adsorbing up to 10 times more Ra than clay (Simon and Ibrahim 1990). Fe- and Mn-oxides (Gonneea et al. 2008; Beck and Cochran 2013) also increase the $K_{\rm d}$ for Ra isotopes. Indeed, the intertidal sediments in Simpson Lagoon have high Fe content based on visual observations and sediment core analyses (Schaal 2024). Finally, since $K_{\rm d}$ is inversely related to

temperature (Rama and Moore 1996; Gonneea et al. 2008), colder temperatures may be contributing to the low ground-water Ra activities compared with more temperate sites.

SGD inputs into Simpson lagoon

We employed the Ra isotope mass balance box model approach to quantify SGD (Moore 1996; Moore and Krest 2004; Garcia-Orellana et al. 2021), using the short-lived isotopes (²²⁴Ra and ²²³Ra) only owing to high background activities for the long-lived isotopes in the Beaufort waters immediately outside the lagoon (Fig. 2, Supporting Information Fig. S1). The relative fraction of daily inputs of ²²⁴Ra and ²²³Ra for all sampling periods are shown in Fig. 4. Detailed discussion of the model and all parameters used can be found in the Supporting Information Data S1.

Conversion of SGD in dpm d⁻¹ to a water flux (m³ d⁻¹) requires a groundwater Ra endmember value in dpm m⁻³. The choice of the Ra endmember value has been extensively debated in the literature (Michael et al. 2011; Luek and Beck 2014; Cho and Kim 2016; Cerdà-Domènech et al. 2017). The maximum Ra values are used to provide conservative, lower-limit SGD estimates in numerous studies (e.g., Moore 1996;

Null et al. 2019); however, we chose to use the 90th percentile Ra activities from each sampling period to lower the impact of extreme outliers.

The SGD rates determined by ²²⁴Ra and ²²³Ra were averaged for each period with the standard deviation taken as the error. Inputs of Ra owing to SGD could not be resolved for June 2022. The two periods with minimal easterly wind input had estimated SGD fluxes of $(22 \pm 8) \times 10^6 \text{ m}^3 \text{ d}^{-1}$ for August 2021 and $(6 \pm 3) \times 10^6 \, \text{m}^3 \, \text{d}^{-1}$ for July 2022. The impact of higher wind speeds during lagoon sampling can be seen in the higher flux from August 2021 (Supporting Information Fig. S5). July 2023 had a high Ra inventory in the lagoon owing to a recent set-down period, but an SGD flux similar to August 2021 and July 2022 at $(12 \pm 4) \times 10^6 \,\mathrm{m}^3 \,\mathrm{d}^{-1}$, presumably owing to the fact that water levels had begun rising at the time of sampling. Finally, October 2022 was sampled directly following a set-down period, before water levels returned to normal. This resulted in not only a high Ra inventory in the lagoon, but also high SGD fluxes coming in at an estimated (79 \pm 16) \times 10⁶ m³ d⁻¹.

The SGD fluxes, which average $(160 \pm 90) \text{ m}^3 \text{ d}^{-1} \text{ m}^{-1}$ of shoreline during the non-easterly wind periods and

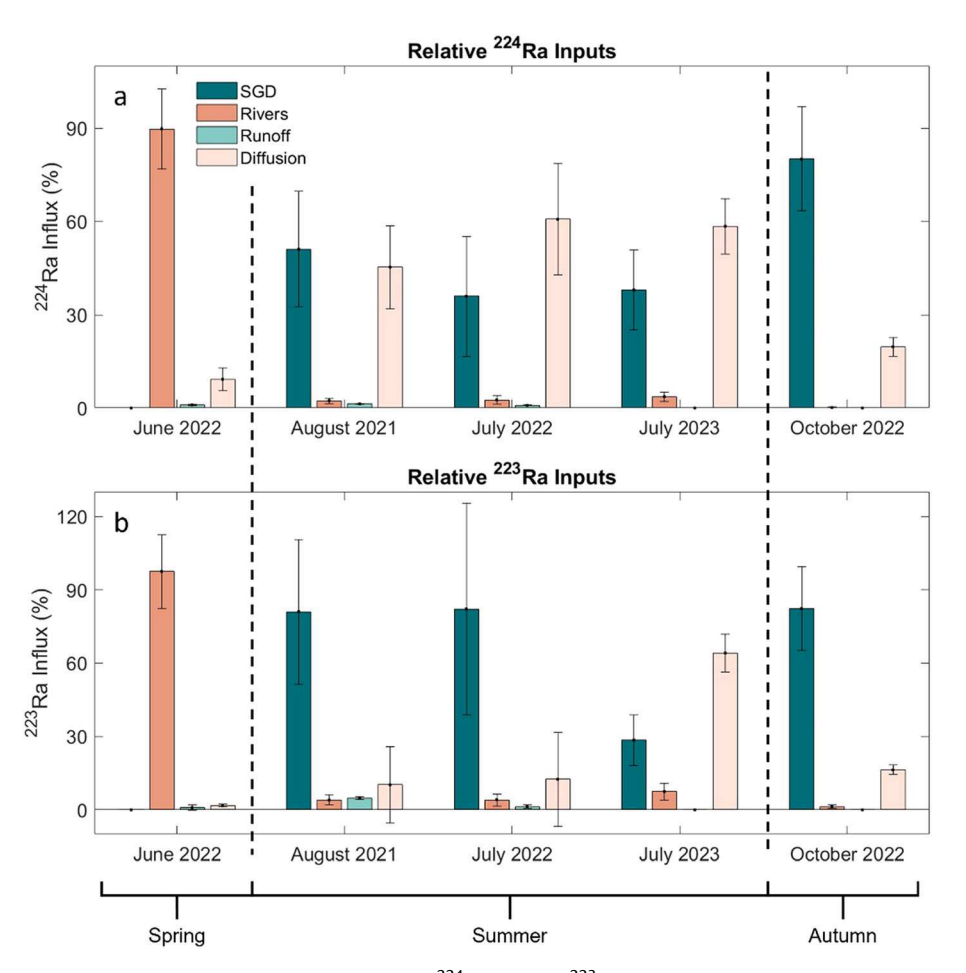


Fig. 4. Relative daily inputs of Ra isotopes by source and season for (a) ²²⁴Ra and (b) ²²³Ra.

 $(890 \pm 200) \text{ m}^3 \text{ d}^{-1} \text{ m}^{-1}$ during the easterly wind period, are on the high range of the few supra-permafrost SGD fluxes reported for the Arctic. Two other sites along the Beaufort Coast reported fluxes of 1.0, 12, and 43 m³ d⁻¹ m⁻¹ of shoreline during summer months (Dimova et al. 2015, Lecher et al. 2015, Connolly et al. 2020). Our SGD estimates are more in line with SGD fluxes reported for southern Alaska, including those seen at Kasitsna Bay (125 m³ d⁻¹ m⁻¹) and Seldovia Slough ([170 \pm 240] m³ d⁻¹ m⁻¹) (Dimova et al. 2015; Lecher et al. 2015). However, unlike these other sites, the SGD in Simpson Lagoon does not seem to be isolated to margin sediments, as indicated by the high Ra activities observed throughout the lagoon (Supporting Information Fig. S1). Benthic exchange was estimated using a wave-pumping model developed by Sawyer et al. (2013). This simplified model shows that the shallow nature of the lagoon and hydraulic conductivities could allow SGD to occur over the full lagoon area (see Supporting Information Data S7). In this case, SGD rates would be $(0.06 \pm 0.04)~\text{m}^3~\text{m}^{-2}~\text{d}^{-1}$ for the noneasterly wind periods, and $(0.3 \pm 0.1) \text{ m}^3 \text{ m}^{-2} \text{ d}^{-1}$ for the easterly wind period.

Demir et al. (submitted) used numerical models and in situ hydrological techniques to derive a freshwater SGD flux into Simpson Lagoon for August 2021 of (0.12–0.14) \times 10⁶ m³ d⁻¹; this is equivalent to \sim 1% of the total SGD flux for that period, which is in the lower range seen at more temperate sites (Tamborski et al. 2015; Cho et al. 2018). This low percentage is likely owing to the inclusion of lagoon water advection through bottom sediments as a component of SGD in our box model, as well as the limited capacity for a terrestrial water table to form, owing to the shallow active layer depth and minimal topographical gradient.

The observations in this study and those reported by Guimond et al. (2023) indicate that wind direction and speed are the dominating drivers of SGD in Simpson Lagoon during ice-free periods, with easterly winds driving higher SGD fluxes. Based on wind direction and strength in late-June through October of 2021, 2022, and 2023 (NOAA 2023), easterly winds that are sustained for a day or more occur 17%–20% of the time. Given that ice and snow cover the land for roughly two-thirds of the year (McClelland et al. 2014), that leaves \sim 120 d (4 months) where SGD can occur. Based on set-down periods occurring 20% of the time and a 4-month ice-free season, our weighted annual SGD flux into Simpson Lagoon is $(3.2\pm1.2)\times10^9~\text{m}^3~\text{y}^{-1}$, which is comparable to the annual flux of the Kuparuk River.

Conclusions

Since Arctic groundwater has been shown to be an important source of carbon and nutrients to an Arctic coastal zone (Connolly et al. 2020), understanding seasonal variability and driving processes are important for tracing its impact on these sensitive coastal systems. This study used the four Ra isotopes

to characterize seasonal SGD inputs to an Arctic coastal lagoon and to investigate Ra dynamics within an Arctic estuarine system. The results showed that SGD is seasonally variable in the Arctic, with limited inputs during spring and inputs dependent on wind conditions during ice-free seasons. However, more research needs to be done to better understand the factors influencing Ra cycling in the Arctic. The interplay between Simpson Lagoon's soil/sediment characteristics, groundwater residence times, and seasonally changing salinity create unique Ra dynamics that appear to be dominated by short-term processes such as temporary water level changes and wind-driven wave pumping; however, this may not hold true along other Arctic coastlines with different topography and sediment properties. As the ice-free season grows longer and weather patterns change owing to Arctic warming, understanding the processes controlling SGD in this environment will become increasingly important.

Data availability statement

The data that support the findings of this study are openly available in the Arctic Data Center at http://doi.org/10.18739/A23B5W945.

References

Beck, A. J., and M. A. Cochran. 2013. Controls on solid-solution partitioning of radium in saturated marine sands. Mar. Chem. **156**: 38–48. doi:10.1016/j.marchem.2013. 01.008

Bristol, E. M., and others. 2021. Geochemistry of coastal permafrost and erosion-driven organic matter fluxes to the Beaufort Sea near drew point, Alaska. Front. Earth Sci. 8. doi:10.3389/feart.2020.598933

Bullock, E. J., L. Kipp, W. Moore, K. Brown, P. J. Mann, J. E. Vonk, N. Zimov, and M. A. Charette. 2022. Radium inputs into the Arctic Ocean from Rivers: A basin-wide estimate. J. Geophys. Res. Oceans 127: e2022JC018964. doi:10.1029/2022JC018964

Cerdà-Domènech, M., V. Rodellas, A. Folch, and J. Garcia-Orellana. 2017. Constraining the temporal variations of Ra isotopes and Rn in the groundwater end-member: Implications for derived SGD estimates. Sci. Total Environ. **595**: 849–857. doi:10.1016/j.scitotenv.2017.03.005

Charette, M. A., K. O. Buesseler, and J. E. Andrews. 2001. Utility of radium isotopes for evaluating the input and transport of groundwater-derived nitrogen to a Cape Cod estuary. Limnol Oceanogr **46**: 465–470. doi:10.4319/lo. 2001.46.2.0465

Charkin, A. N., and others. 2017. Discovery and characterization of submarine groundwater discharge in the Siberian Arctic seas: A case study in the Buor-khaya gulf, Laptev Sea. Cryosphere **11**: 2305–2327. doi:10.5194/tc-11-2305-2017

- Cho, H.-M., and G. Kim. 2016. Determining groundwater Ra endmember values for the estimation of the magnitude of submarine groundwater discharge using Ra isotope tracers. Geophys. Res. Lett. **1-7**: 3865–3871. doi:10.1002/2016GL068805
- Cho, H.-M., G. Kim, E. Y. Kwon, N. Moosdorf, J. Garcia-Orellana, and I. R. Santos. 2018. Radium tracing nutrient inputs through submarine groundwater discharge in the global ocean. Sci. Rep. **8**: 2439. doi:10.1038/s41598-018-20806-2
- Connolly, C. T., M. B. Cardenas, G. A. Burkart, R. G. M. Spencer, and J. W. McClelland. 2020. Groundwater as a major source of dissolved organic matter to Arctic coastal waters. Nat. Commun. **11**: 1479. doi:10.1038/s41467-020-15250-8
- Deming, D., J. H. Sass, A. H. Lachenbruch, and R. F. De Rito. 1992. Heat flow and subsurface temperature as evidence for basin-scale ground-water flow, north slope of Alaska. Geo. Soc. Am. Bull. **104**: 528–542.
- Dimova, N. T., A. Paytan, J. D. Kessler, K. J. Sparrow, F. G.-T. Kodovska, A. L. Lecher, J. Murray, and S. M. Tulaczyk. 2015. Current magnitude and mechanisms of groundwater discharge in the Arctic: Case study from Alaska. Environ. Sci. Tech. **49**: 12036–12043. doi:10.1021/acs.est. 5b02215
- Déry, S. J., M. Stieglitz, Å. K. Rennermalm, and E. F. Wood. 2005. The water budget of the Kuparuk River basin, Alaska. J. Hydrometer. **6**: 633–655.
- Frederick, J. M., and B. A. Buffett. 2015. Effects of submarine groundwater discharge on the present day extent of relict submarine permafrost and gas hydrate stability on the Beaufort Sea continental shelf. Case Rep. Med. **120**: 417–432. doi:10.1002/2014JF003349
- Garcia-Orellana, J., and others. 2021. Radium isotopes as submarine groundwater discharge (SGD) tracers: Review and recommendations. Earth Sci. Rev. **220**: 103681. doi:10. 1016/j.earscirev.2021.103681
- Gonneea, M. E., P. J. Morris, H. Dulaiova, and M. A. Charette. 2008. New perspectives on radium behavior within a subterranean estuary. Mar. Chem. **109**: 250–267. doi:10.1016/j.marchem.2007.12.002
- Guimond, J. A., C. Demir, B. L. Kurylyk, M. A. Walvoord, J. W. McClelland, and M. B. Cardenas. 2023. Wind-modulated groundwater discharge along a microtidal Arctic coastline. Environ. Res. Lett. 18: 94042. doi:10.1088/1748-9326/acf0d8
- Hanna, A. J. M., T. M. Shanahan, M. A. Allison, T. S. Bianchi, and K. M. Schreiner. 2018. A multi-proxy investigation of late-Holocene temperature change and climate-driven fluctuations in sediment sourcing: Simpson lagoon, Alaska. Holocene 28: 984–997. doi:10.1177/0959683617752845
- IPCC. 2021. Climate change 2021: The physical science basis. *In* V. Masson-Delmotte and others [eds.], Contribution of working group I to the sixth assessment report of the

- intergovernmental panel on climate change. Cambridge University Press.
- Key, R. M., N. L. Guinasso, and D. R. Schink. 1979. Emanation of radon-222 from marine sediments. Mar. Chem. **7**: 221–250. doi:10.1016/0304-4203(79)90041-0
- Key, R. M., R. F. Stallard, W. S. Moore, and J. L. Sarmiento. 1985. Distribution and flux of ²²⁶Ra and ²²⁸Ra in the Amazon River. J. Geophys. Res. **90**: 6995–7004.
- Kipp, L. E., P. B. Henderson, Z. A. Wang, and M. A. Charette. 2020. Deltaic and estuarine controls on Mackenzie River solute fluxes to the Arctic Ocean. ESCO 43: 1992–2014. doi:10.1007/s12237-020-00739-8
- Lecher, A. L. 2017. Groundwater discharge in the Arctic: A review of studies and implications for biogeochemistry. Hydrology **4**: 41. doi:10.3390/hydrology4030041
- Lecher, A. L., C.-T. Chien, and A. Paytan. 2016. Submarine groundwater discharge as a source of nutrients to the North Pacific and Arctic coastal ocean. Mar. Chem. **186**: 167–177. doi:10.1016/j.marchem.2016.09.008
- Lecher, A. L., J. Kessler, K. Sparrow, F. G.-T. Kodovska, N. Dimova, J. Murray, S. Tulaczyk, and A. Paytan. 2015. Methane transport through submarine groundwater discharge to the North Pacific and Arctic Ocean at two Alaskan sites. L&O **61**: S344–S355. doi:10.1002/lno.10118
- Linhoff, B. S., M. S. Charette, and J. Wadham. 2020. Rapid mineral surface weathering beneath the Greenland ice sheet shown by radium and uranium isotopes. Chem. Geo. **547**: 119663. doi:10.1016/j.chemgeo.2020.119663
- Luek, J. L., and A. J. Beck. 2014. Radium budget of the York River estuary (VA, USA) dominated by submarine groundwater discharge with a seasonally variable groundwater end-member. Mar. Chem. **165**: 55–65. doi:10.1016/j. marchem.2014.08.001
- McClelland, J. W., A. Townsend-Small, R. M. Holmes, F. Pan, M. Stieglitz, M. Khosh, and B. J. Peterson. 2014. River export of nutrients and organic matter from the north slope of Alaska to the Beaufort Sea. Water Resour. Res. **50**: 1823–1839. doi:10.1002/2013WR014722
- Michael, H. A., M. A. Charette, and C. F. Harvey. 2011. Patterns and variability of groundwater flow and radium activity at the coast: A case study from Waquoit Bay. Mar. Chem. **127**: 100–114. doi:10.1016/j.marchem.2011.08.001
- Moore, W. S. 1996. Large groundwater inputs to coastal waters revealed by ²²⁶Ra enrichments. Nature **380**: 612–614. doi: 10.1038/380612a0
- Moore, W. S. 1998. Application of ²²⁶Ra, ²²⁸Ra, ²²³Ra, and ²²⁴Ra in coastal waters to assessing coastal mixing rates and groundwater discharge to oceans. Proc. Indian Natl. Sci. Acad. **107**: 343–349.
- Moore, W. S. 2008. Fifteen years experience in measuring 224Ra and 223Ra by delayed coincidence counting. Mar. Chem. **109**: 188–197.
- Moore, W. S. 2010. The effect of submarine groundwater discharge on the ocean. Ann. Rev. Mar. Sci. **2**: 59–88. doi:10. 1146/annurev-marine-120308-081019

- Moore, W. S., and J. Krest. 2004. Distribution of ²²³Ra and ²²⁴Ra in the plumes of the Mississippi and Atchafalaya Rivers and the Gulf of Mexico. Mar. Chem. **86**: 105–119.
- NOAA: Station PRDA2-9497645-Prudhoe Bay, AK. 2023. National Data Buoy Center. NOAA, [accessed 2024 Jan 12]. Available from https://www.ndbc.noaa.gov/station_page.php?station=prda2
- Null, K. A., D. R. Corbett, J. Crenshaw, R. N. Peterson, L. E. Peterson, and W. B. Lyons. 2019. Groundwater discharge to the western Antarctic coastal ocean. Polar Res. **38**. doi:10. 33265/polar.v38.3497
- Rama, and W. S. Moore. 1996. Using the radium quartet for evaluating groundwater input and water exchange in salt marshes. Geo. Cosmochim. Acta **60**: 4645–4652.
- Rantanen, M., A. Y. Karpechko, A. Lipponen, K. Nordling, O. Hyvärinen, K. Ruosteenoja, T. Vihma, and A. Laaksonen. 2022. The Arctic has warmed nearly four times faster than the globe since 1979. Comm. Earth Environ. **3**: 168. doi:10. 1038/s43247-022-00498-3
- Santos, I. R., B. D. Eyre, and M. Huettel. 2012. The driving forces of porewater and groundwater flow in permeable coastal sediments: A review. Est. Coast. Shelf Sci. **98**: 1–15. doi:10.1016/j.ecss.2011.10.024
- Sawyer, A. H., F. Shi, J. T. Kirby, and H. A. Michael. 2013. Dynamic response of surface water-groundwater exchange to currents, tides, and waves in a shallow estuary. J. Geophys. Res. Oc. 118: 1749–1758. doi:10.1002/jgrc. 20154
- Schaal, I. V. 2024. Distribution and behavior of trace metals in the subterranean estuary of an Arctic coastal lagoon. Master's Thesis. Massachusetts Institute of Technology.
- Scholten, J. C., M. K. Pham, O. Blinova, M. A. Charette, H. Dulaiova, and M. Eriksson. 2010. Preparation of Mn-fiber standards for the efficiency calibration of the delayed coincidence counting system (RaDeCC). Mar. Chem. **121**: 206–214. doi:10.1016/j.marchem.2010.04.009
- Simon, S. L., and S. A. Ibrahim. 1990. Biological uptake of radium by terrestrial plants. In: The Environmental Behaviour of Radium, Technical Report Series, v. **310**. IAEA, p. 545–599.
- Tamborski, J. J., A. D. Rogers, H. J. Bokuniewicz, J. K. Cochran, and C. R. Young. 2015. Identification and quantification of

- diffuse fresh submarine groundwater discharge via airborne thermal infrared remote sensing. Remote. Sens. Environ. **171**: 202–217.
- USDA. 2022. Precipitation, accumulated, Prudhoe Bay, AK. Natural Resources Conservation Service and National Water and Climate Center. USDA, [accessed 2023 April 6]. Available from https://wcc.sc.egov.usda.gov/nwcc/site?sitenum=1177
- USGS: 15875000 Colville R AT Umiat AK. 2023. National Water Information System Data (USGS Water Data for the Nation). USGS, [accessed 2024 January 12]. Available from https://waterdata.usgs.gov/monitoring-location/15875000/#parameterCode=00065&period=P7D
- USGS: Kuparuk R NR Deadhorse AK. 2023. National Water Information System Data (USGS Water Data for the Nation). USGS, [accessed 2023 March 22]. Available from https://waterdata.usgs.gov/nwis/inventory/?site_no=15896000
- van der Loeff, M. R., S. Kühne, M. Wahsner, H. Höltzen, M. Frank, B. Ekwurzel, M. Mensch, and V. Rachold. 2003. ²²⁸Ra and ²²⁶Ra in the Kara and Laptev seas. Cont. Shelf Res. **23**: 113–124. doi:10.1016/S0278-4343(02)00169-3
- Webster, I. T., G. J. Hancock, and A. S. Murray. 1995. Modeling the effect of salinity on radium desorption from sediments. Geo. Cosmochim. Acta **59**: 2469–2476.

Acknowledgments

This project was funded by the National Science Foundation's Office of Polar Programs through grants 1938873 (Charette), 1938820 (Cardenas and McClelland), and 1656026 (McClelland). Assistance with fieldwork and data interpretation was provided by Cansu Demir, Julia Guimond, and Emily Bristol. We thank Hillcorp Alaska for providing access to field sites and Battelle Arctic Research Operations (via Polar Field Services) for logistical support. We also thank the Beaufort Lagoon Ecosystems Long Term Ecological Research program for sharing lab and field resources.

Conflict of Interest

None declared.

Submitted 27 September 2023 Revised 12 April 2024 Accepted 21 April 2024

Associate editor: Perran Cook